

THE SUN AT MINIMUM ACTIVITY: RESULTS FROM THE CELIAS EXPERIMENT ON SOHO

P. Bochsler¹, D. Hovestadt¹, H. Grünwaldt¹, M. Hilchenbach¹, F.M. Ipavich², M.R. Aellig¹, W.I. Axford⁴, H. Balsiger¹, A. Bogdanov³, A. Bürgi³, M.A. Coplan², A.B. Galvin², J. Geiss¹, F. Gliem⁵, G. Gloeckler², S. Heftri¹, K.C. Hsieh⁶, D.L. Judge⁷, R. Kallenbach¹, B. Klecker², H. Kucharek², S.E. Lasley², M.A. Lee⁸, Yu. Litvinenko⁸, S. Livi¹, G.G. Managadze⁹, E. Marsch¹, E. Möbius⁸, M. Neugebauer¹⁰, H.S. Ogawa⁷, J.A. Paquette², K.-U. Reiche⁵, M. Scholer³, M.I. Verigin⁹, B. Wilken⁴, and P. Wurz¹

¹Physikalisches Institut, University of Bern, CH-3012 Bern, Switzerland

²Dept. of Physics and Astronomy, University of Maryland, College Park, MD 20742, USA

³Max-Planck-Institut für Extraterrestrische Physik, D-85740, Garching, Germany

⁴Max-Planck-Institut für Aeronomy, D-37189 Katlenburg-Lindau, Germany

⁵Institut für Datenverarbeitungsanlagen, Technische Universität, D-38023 Braunschweig, Germany

⁶Department of Physics, University of Arizona, Tucson, AZ 85721, USA

⁷Space Science Center, University of Southern California, Los Angeles, CA 90089, USA

⁸EOS, University of New Hampshire, Durham, NH 03824, USA

⁹Institute for Space Physics, Moscow, Russia

¹⁰Jet Propulsion Laboratory, Pasadena, CA 91103, USA

ABSTRACT

CELIAS is a particle experiment which continuously observes the chemical, isotopic, and ionic composition of minor elements in the solar wind. The Proton Monitor of CELIAS provides information on basic plasma parameters such as proton velocity, kinetic temperature, density and the out-of-ecliptic flow angle. A preliminary statistical analysis of proton parameters and freeze-in temperatures obtained during the first 18 months of operation of SOHO at a period of solar minimum activity is presented. The first determinations of neon isotopic abundances with CELIAS yielded an excellent agreement with earlier measurements with the Apollo-Foil Experiment. The magnesium isotopic composition in the solar wind agrees with the terrestrial value. The charge state determination of minor ions with CTOF is carried out with a time resolution of five minutes allowing the study of small scale features in the solar wind flow which might become important for the interpretation of correlated observations with optical instruments. HSTOF and STOF have yielded new and valuable information on energetic heliospheric neutral hydrogen.

INTRODUCTION

The purpose of this paper is to give an overview over the quality of CELIAS data gathered during the first 18 months of SOHO operation. We also discuss a few applications with relevance to solar and coronal physics. The coverage of the energy- and mass-field by CELIAS and a typical solar particle distribution within this field is depicted in Figure 1.

The main purpose of CELIAS is to continuously measure the elemental, isotopic and charge state composition of the solar wind and of solar suprathermal particles and to determine the dynamical properties of minor ions. A detailed description of the different sensors has been published elsewhere (Hovestadt et al. 1995).

CELIAS Energy- and Mass-Ranges

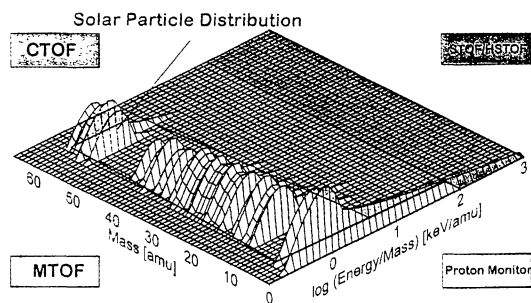


Figure 1: Energy- and Mass-Ranges of CELIAS on SOHO. The grid shows a typical solar wind particle distribution at a bulk drift speed of 400 km/s. Counts are plotted in the third dimension in a logarithmic scale. The elongated tails to the high-energy end illustrate the distributions of suprathermal particles which are associated with flare events and corotating interaction regions. Coloured fields delineate the ranges of the different sensors of CELIAS: Green is for CTOF, red for MTOF and the Proton Monitor, blue is the field of STOF and HSTOF.

PROTON MONITOR: AUTOCORRELATION ANALYSIS OF DYNAMIC PROPERTIES OF PROTONS AND FREEZING-IN TEMPERATURES NEAR SOLAR MINIMUM

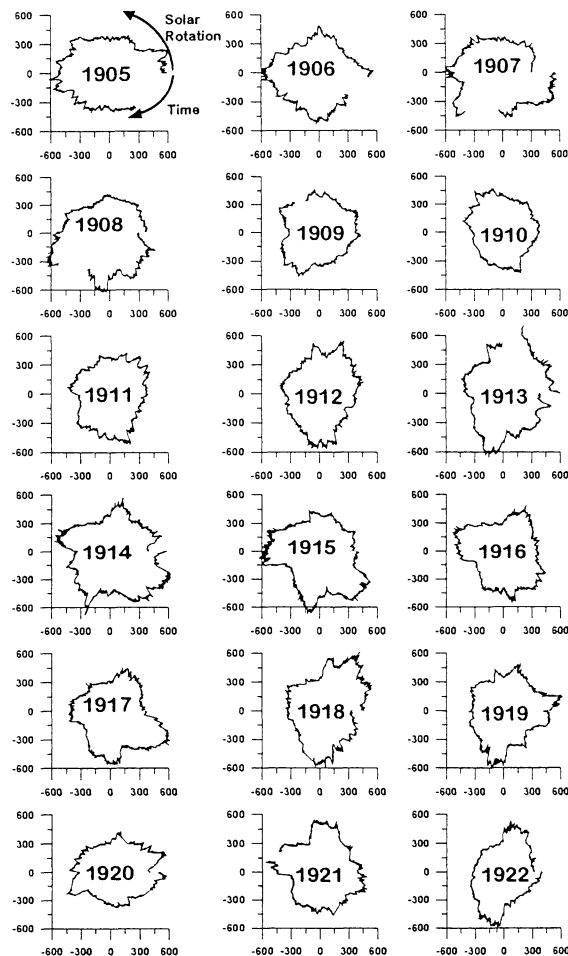


Figure 2: Carrington plots of proton velocities for Carrington rotations 1905-1922 (Jan 1996 - May 1997). The scales are in km/s. In each polar plot the Carrington longitude $360^\circ = 0^\circ$ is at $v_y=0$ on the right hand side (3 o'clock). Time progresses in clockwise rotation, Carrington longitudes increase in counter-clockwise rotation.

Usually, the interplanetary medium exhibits the well-known four-sector structure during solar minimum. This can be interpreted in terms of the simple picture of a tilted solar magnetic dipole or of a warped magnetic solar equator. In an idealized situation near solar minimum the SOHO platform, practically at rest in the ecliptic plane, will therefore experience two crossings of the solar magnetic equator per solar rotation and the

imprint of two solar wind streams originating from higher latitudes, one southern stream and one northern. Figure 2 illustrates that such a situation occurred during CR1905, CR 1912, and CR 1922. The corresponding panels show two pronounced elongations of solar wind speeds reaching 600 km/s. On the other hand, CR 1909, 1910 and 1911 exhibit circular or irregular shapes with no clear indication of a four sector pattern. It is also evident from these figures that the Carrington longitude of the streams remains unchanged for at most two or three rotations and that it is difficult to recognize similarities for two periods as far apart as CR 1905 and CR 1912.

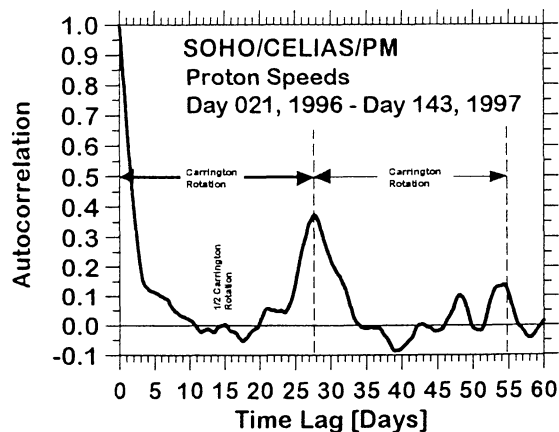


Figure 3: Autocorrelation function of proton speeds observed with CELIAS/PM (full period)

The autocorrelation analysis of proton speeds (Figure 3) shows a pronounced peak at a level of 0.373 after one Carrington rotation and, correspondingly, another maximum at $0.373^2 = 0.139$ after two rotations. Furthermore, the four-sector-structure in the interplanetary medium produces a small intermediate peak after approximately half a solar rotation. This intermediate peak is somewhat more pronounced if only data from 1996 are included, when the four-sector structure was apparently better organized. There is no explanation, however, for the peak at 21 days lag and an even more pronounced peak at 48 days.

The short-time autocorrelation (Figure 4) of proton speeds follows very closely an exponential decay with a characteristic time of 2.3 days. Kinetic temperatures and fluxes of protons show considerably shorter persistence times. Although the freeze-in temperatures, derived from the O^{7+}/O^{6+} abundance ratio (for more details on freeze-in temperatures see Aellig et al. 1997, this volume), show a repetitive peak after one solar rotation, their autocorrelation drops rather rapidly on short time-scales of 12 hours. It seems natural that the parameter

parameter which characterizes the dominant energy carrying feature is the most persistent parameter of the interplanetary medium. The other dynamical parameters, density and kinetic temperature, seem to be much more subdue to modifications by stream-stream interactions in the interplanetary medium, consequently their persistence times are considerably shorter.

An open question remains with the short persistence time of freeze-in temperatures. We have recently emphasized (Aellig et al. 1997, Hefti et al. 1997) that freeze-in temperatures are good indicators for conditions in the inner corona, and that this parameter is not modified during transport from the freeze-in location near $1 R_{\odot}$ to 1 AU. Nevertheless, its persistence time shown in Figure 5 is rather short, although some recurrence peak (not shown here) is observed after a full solar rotation. In view of this observation one must refine the above argumentation about the causes of the long persistence time of proton speeds at 1 AU.

Probably, variations of proton speeds occur in a very similar manner as do variations of freeze-in temperatures at short distances from the Sun. Despite the fact that proton speeds are quite insensitive to stream-stream interactions, some smoothing of high frequency features occur, such that only low frequency properties survive as far out as 1 AU.

In summary, there are probably two causes which cause the long persistence time of proton speeds:

- (A) Smoothing of small scale features, and
- (B) enhanced stability of features with high specific energy content.

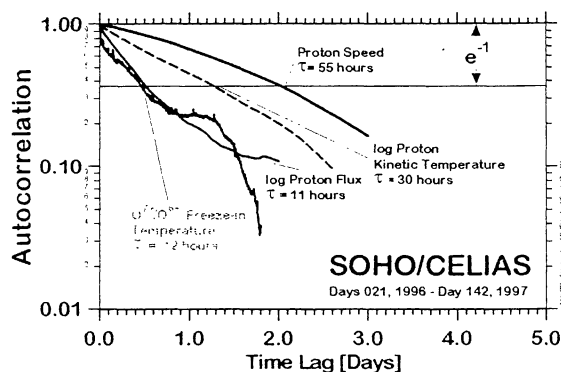


Figure 4: Persistence of proton dynamic properties and of oxygen freeze-in temperatures. The characteristic time scales are estimated from a linear fit to the logarithms of the autocorrelations functions.

CTOF: FREEZE-IN TEMPERATURES IN SMALL-SCALE STRUCTURES

Figure 5 (Hefti et al. 1997) is an overview in the mass vs. mass per charge space covering 50 days of data collected with the CTOF sensor. CTOF is a linear time of flight mass-spectrometer with a large geometrical factor. Thanks to the three-axis stabilization of the SOHO-platform the duty cycle of the instrument is practically 100%. The entrance system of CTOF contains a hemispherical energy analyzer which is combined with two quadrupole lenses which provide a wide angular acceptance in the directions perpendicular to the flow axis. The entrance system is thus covering the full phase space occupied by solar wind particles with a very smooth dependence of the transmission function on angles. This instrumental property minimizes an often encountered difficulty in composition analysis of space plasmas: Incomplete coverage of phase space, or coverage with variable sensitivity and variable calibration factors, generates ambiguity, even for such simple parameters as abundance ratios of charge states of the same element. Due to the post-acceleration voltage between the entrance system and the time-of-flight sensor, variations in sensitivity caused by variable bulk speeds are strongly reduced.

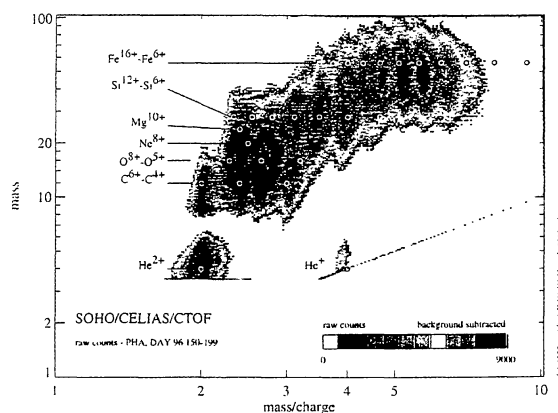


Figure 5: Fifty days of data registered with CELIAS/CTOF (from Hefti et al., 1997)

Wimmer-Schweingruber et al. (1997) have used freeze-in temperatures and Mg/O abundance ratios to identify stream interfaces in corrotating interaction regions with data from Ulysses/SWICS. The large geometrical factor of CTOF and the high resolving power of the sensor result in an unprecedented time resolution. This is important for correlative studies with optical observations and for backmapping of streams to their origins on the solar surface. Events with variations on short time scales have recently been analysed in detail by Hefti et al. (1997). Figure 6 is an impressive example in

O^{7+}/O^{6+} -freeze-in temperature (T_{76}) in the solar wind drops practically within ten minutes from a previously stable level near $1.5 \cdot 10^6$ K to a lower level around $1.2 \cdot 10^6$ K, clearly indicating the location of the interface. Identification of this interface is much more difficult from the dynamical parameters such as proton speed or proton density.

Another illustration of a stream interface which can readily be identified by means of the O^{7+}/O^{6+} -freeze-in

SOHO/CELIAS DAYS 157/158, 1996

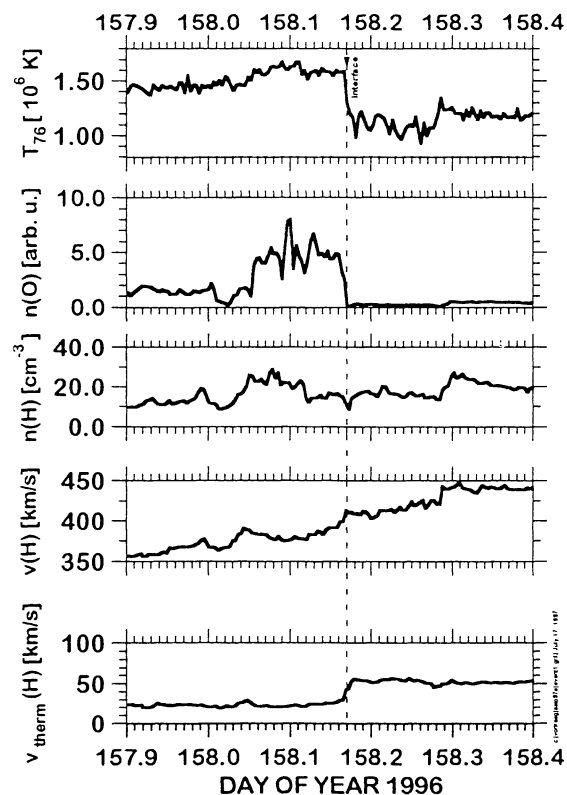


Figure 6: (from Hefti et al. 1997) Identification of an interface between low speed solar wind and a stream at elevated speed. The proton speed increases gradually within 12 hours from 350 km/s to 450 km/s. The interaction of the intermediate speed stream with the low speed solar wind seems to produce a compression of the oxygen density which is, however, not clearly identified in the hydrogen density. The kinetic temperature remains low in the compression region and increases only in the intermediate stream. The clearest separation between the two regimes is possible using T_f (O^{7+}/O^{6+}) (topmost panel). This parameter drops by 300'000 K within a short interval of 10 minutes.

temperature is Figure 7. In this case a smooth transition from intermediate speed solar wind to low speed solar wind is seen in the parameter $v(H)$. There is no clear distinction between the two adjacent streams in the dynamical parameters $n(H)$, $n(O)$, $v_{\text{therm}}(H)$, and $v(H)$. The freeze-in temperature, however, steeply increases by approximately 300'000 K around day 191.53, clearly separating two different streams which are otherwise indistinguishable.

SOHO/CELIAS DAY 191, 1996

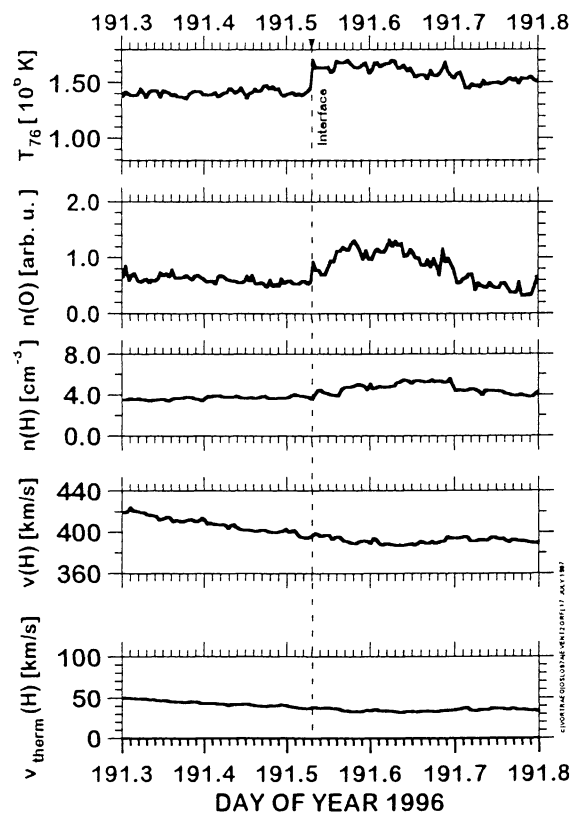


Figure 7: (from Hefti et al. 1997). Identification of a stream interface in a period of gradual transition from intermediate speed solar wind to low speed solar wind. The step in freeze-in temperatures (top panel) indicates how well this interface must have been conserved between two adjacent streams during the transit of more than four days from the freeze-in event at $\sim 1 R_{\odot}$ to 1 AU.

MTOF: FIRST RESULTS ON ISOTOPIC ABUNDANCE DETERMINATIONS

MTOF considerably expands the database of well-studied elements and isotopes in the solar wind. An example of a summed mass spectrum is shown in

Figure 8. Many of the newly identified elements in the solar wind have very low first ionization potentials and their abundances in different solar wind regimes will provide crucial tests for the different models of the ion-neutral separation mechanism. Isotopic abundances of non-volatile elements can be used to test the authenticity of solar wind samples for the isotopic composition of the outer convective zone of the Sun and for the extent of secular gravitational settling within the outermost layers of the Sun.

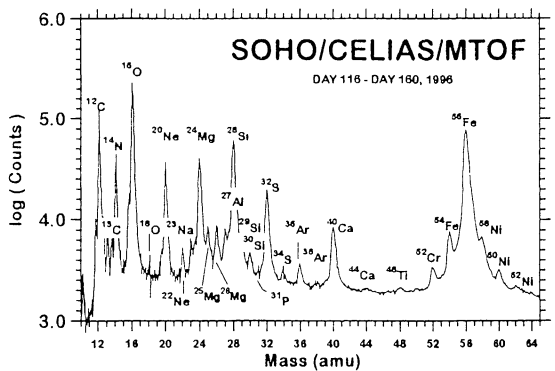


Figure 8: Mass spectrum accumulated with MTOF/CELIAS. Many of the elements and isotopes indicated in this spectrum have been identified for the first time in the solar wind with MTOF.

Solar Isotopic Abundances 1997
Results from CELIAS/MTOF and from WIND/MASS

					Si 25	Si 26	Si 27	Si 28	Si 29	Si 30
					Al 23	Al 24	Al 25	Al 26	Al 27	Al 28
					Mg 20	Mg 21	Mg 22	Mg 23	Mg 24	Mg 25
					Na 20	Na 21	Na 22	Na 23	Na 24	Na 25
					Ne 17	Ne 18	Ne 19	Ne 20	Ne 21	Ne 22
					F 17	F 18	F 19	F 20	F 21	F 22
					O 14	O 15	O 16	O 17	O 18	O 19
					N 13	N 14	N 15	N 16	N 17	N 18
					C 12	C 13	C 14	C 15	C 16	C 17

Figure 9: Solar wind isotopic abundances derived from WIND/MASS and from SOHO/CELIAS/MTOF. In the low mass range several geochemically relevant isotopes of volatile elements such as N and C have not yet been determined until now.

For the volatile elements, solar wind isotopic abundances are the only source of information on the solar isotopic composition which is itself the point of reference for the origin and the evolution of the solar system. The solar atmosphere is also the only authentic sample of galactic interstellar matter as it existed 4.6 Gy ago

when the solar system finally separated from the dense molecular cloud in which it originated.

Thus far the isotopic composition of neon (Kallenbach et al. 1997) and of magnesium (Kucharek et al. 1997, this volume) have been derived from MTOF data. A compilation of solar wind isotopic abundances measured with WIND/MASS (Collier et al., 1997; Wimmer-Schweingruber et al. 1997) and with SOHO/CELIAS/MTOF is presented in Figure 9.

STOF/HSTOF: DETECTION OF ENERGETIC NEUTRAL HYDROGEN OF HELIOSPHERIC ORIGIN

Energetic neutral atoms (ENAs) are produced through charge-exchange of energetic particles with neutrals from interstellar gas penetrating into the heliosphere, from the interaction of solar energetic particles with cool solar ejecta, and from charge exchange of energetic particles with planetary atmospheric atoms.

HSTOF is a mass and energy analyzer combining time-of-flight measurement with residual energy determination which makes it possible to identify masses of incoming particles. The entrance system of STOF/HSTOF consists of two sections. The larger part is a stack of cylindrically shaped energy analyzer plates which allow the determination of the energy per charge of incoming particles. Adjacent to this section and also giving access to the time-of-flight sensor is a stack of charged flat parallel plates on alternative potentials of + and - 4.5 kV. This second stack serves as a filter for charged particles with energies below 70 keV/e. Neutral particles are admitted from a field of view of $\pm 2^\circ$ by $\pm 17^\circ$.

The comparison of charged particle fluxes measured with STOF and of charged *and neutral particles* in the same energy range from 50 to 100 keV detected with HSTOF and shown in Figure 10, makes it possible to distinguish neutral particle fluxes from charged particle fluxes.

Hsieh et al. (1997) investigate the temporal trend of energetic neutrals and find no 27 day recurrence. From the preliminary evidence they tentatively conclude that the most important source of energetic neutral hydrogen (ENH) near the solar minimum is not solar (e.g. SEPs, CMEs etc.). However, they notice a conspicuous peak of ENHs near day 200 of 1996. This peak coincides with the period when the Earth is upstream in the interstellar medium relative to the Sun and in the direction of the putative heliospheric termination shock. Whether a heliospheric shock is really the source of the

detected ENHs needs to be confirmed during the period when the Earth will be at the same location relative to the Sun in 1997.

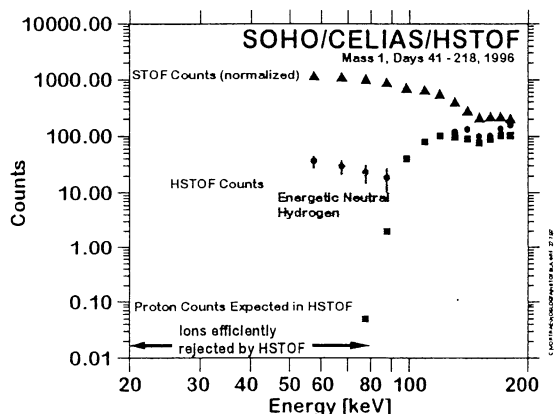


Figure 10: (adapted from Hsieh et al. 1997) Comparison of HSTOF and STOF data during quiet periods in 1996. The circles indicate the total counts registered with HSTOF, the triangles show the normalized total proton counts registered with STOF during the same periods. At high energies count rates of STOF and HSTOF coincide. At low energies the HSTOF efficiently discriminates charged particles. This is shown with the low rates of expected counts inferred from STOF rates for HSTOF which are indicated by squares in this diagram. It is concluded that the counts observed in the shaded area are predominantly due to energetic neutral hydrogen.

SUMMARY AND CONCLUSION

Since its launch in December 1995 CELIAS has established an important link in solar-terrestrial physics. The Proton Monitor which was originally conceived as an auxiliary sensor for the operation of MTOF, has meanwhile become an indispensable source of information for applications in space research. Solar wind parameters derived from Proton Monitor data are available near-real-time on the World Wide Web (<http://umtof.umd.edu/pm>). The CTOF-sensor has provided compositional data with unprecedented sensitivity and time resolution. MTOF together with its twin, the MASS-sensor on WIND, has led to the first detection of a large set of new elements and isotopes in the solar wind. STOF/HSTOF is gathering information on solar suprathermal and energetic particles. Although the fluxes of energetic particles are rather low during the present phase of the solar cycle, a first identification of energetic neutrals has been possible. The heliospheric shock has tentatively been identified as a source of these particles.

ACKNOWLEDGMENTS

The authors gratefully acknowledge the contributions of the many individuals in the CELIAS Team and of ESA and NASA who contributed to the success of SOHO.

REFERENCES

- Aellig M.R., Grünwaldt H., Bochsler P., Wurz P., Hefti S., Kallenbach R., Ipavich F.M., Hovestadt D., Hilchenbach M., and the CELIAS Team (1997) Solar wind iron charge states observed with high time resolution with CELIAS/CTOF. **Proceedings of the Fifth SOHO Workshop, OSLO** (this volume).
- Collier M.R., Hamilton D.C., Gloeckler G., Ho G., Bochsler P., and Sheldon R.B. (1997) The oxygen-16 to oxygen-18 abundance ratio in the solar wind observed with WIND/MASS. (preprint)
- Hefti S., Bochsler P., Aellig M., Kallenbach R., Wurz P., Grünwaldt H., Hilchenbach M., Hovestadt D., and Ipavich F.M. (1997) Oxygen freeze-in temperature measured by SOHO/CELIAS (Abstract). **EOS 78, S254**.
- Hovestadt D., Hilchenbach M., Bürgi A., Klecker B., Laeverenz P., Scholer M., Grünwaldt H., Axford W.I., Livi S., Marsch E., Wilken B., Winterhoff H.P., Ipavich F.M., Bedini P., Coplan M.A., Galvin A.B., Gloeckler G., Bochsler P., Balsiger H., Fischer J., Geiss J., Kallenbach R., Wurz P., Reiche K.-U., Gliem F., Judge D.L., Ogawa H.S., Hsieh K.C., Möbius E., Lee M.A., Managadze G.G., Verigin M.I., and Neugebauer M. (1995) CELIAS - Charge, Element and Isotope Analysis System for SOHO. **Solar Physics 162, 441 - 481**.
- Hsieh K.C., Hilchenbach M., Bochsler P., Hovestadt D., Grünwaldt H., Ipavich F.M., Axford W.I., Balsiger H., Bürgi A., Coplan M.A., Galvin A.B., Geiss J., Gliem F., Gloeckler G., Judge D.L., Kallenbach R., Klecker B., Lee M.A., Livi S., Managadze G.G., Marsch E., Möbius E., Neugebauer M., Ogawa H.S., Reiche K.-U., Scholer M., Verigin M.I., Wilken B., Wurz P. (1997) Energetic neutral hydrogen atoms of heliospheric origin detected with SOHO/CELIAS - an update (Abstract). **EOS 78, S260**.
- Kallenbach R., Ipavich F.M., Bochsler P., Hefti S., Hovestadt D., Grünwaldt H., Hilchenbach M., Axford W.I., Balsiger H., Bürgi A., Coplan M.A., Galvin A.B., Geiss J., Gliem F., Gloeckler G., Hsieh K.C., Klecker B., Lee M.A., Livi S., Managadze G.G., Marsch E.,

Möbius E., Neugebauer M., Reiche K.-U., Scholer M., Verigin M.I., Wilken B., Wurz P. (1997) Isotopic composition of solar wind neon measured by CELIAS/M-TOF onboard SOHO. **J. Geophys. Res.** (in press).

Kucharek H., Ipavich F.M., Kallenbach R., Gliem F., Grünwaldt H., Hilchenbach M., Klecker B., Bochsler P., Hovestadt D. and the CELIAS Team. (1997) Magnesium isotopes in the solar wind with CELIAS/M-TOF. **Proceedings of the Fifth SOHO Workshop, OSLO** (this volume).

Wimmer-Schweingruber R.F., Kern O., Bochsler P., Bodmer R., Gloeckler G., and Hamilton D.C. (1997) First determination of the solar silicon isotopic composition: WIND/MASS results. (Abstract) **EOS, S 254**.

Wimmer-Schweingruber R.F., von Steiger R., and Paerli R. (1997) Solar wind stream interfaces in corrotating interaction regions. SWICS/Ulysses results. **J. Geophys. Res.** (in press).